PLOS ONE

RESEARCH ARTICLE

Measurement of Inositol 1,4,5-Trisphosphate in Living Cells Using an Improved Set of Resonance Energy Transfer-Based Biosensors

Gergő Gulyás[1☯], József T. Tóth[1☯], Dániel J. Tóth[1], István Kurucz[2], László Hunyady[1], Tamas Balla[2], Péter Várnai[1]*

1 Department of Physiology, Faculty of Medicine, Semmelweis University, Budapest 1094, Hungary, **2** Section on Molecular Signal Transduction, Program for Developmental Neuroscience, National Institute of Child Health and Human Development, National Institutes of Health, Bethesda, MD 20892, United States of America

☯ These authors contributed equally to this work.
* varnai.peter@med.semmelweis-univ.hu

CrossMark
click for updates

OPEN ACCESS

Citation: Gulyás G, Tóth JT, Tóth DJ, Kurucz I, Hunyady L, Balla T, et al. (2015) Measurement of Inositol 1,4,5-Trisphosphate in Living Cells Using an Improved Set of Resonance Energy Transfer-Based Biosensors. PLoS ONE 10(5): e0125601. doi:10.1371/journal.pone.0125601

Academic Editor: Mohamed Trebak, Penn State Hershey College of Medicine, UNITED STATES

Received: January 16, 2015

Accepted: March 24, 2015

Published: May 1, 2015

Copyright: This is an open access article, free of all copyright, and may be freely reproduced, distributed, transmitted, modified, built upon, or otherwise used by anyone for any lawful purpose. The work is made available under the Creative Commons CC0 public domain dedication.

Data Availability Statement: All relevant data are within the paper.

Funding: Funding provided by Hungarian Scientific Research Fund (OTKA) K105006: PV, http://www.otka.hu/en.

Competing Interests: The authors have declared that no competing interests exist.

Abstract

Improved versions of inositol-1,4,5-trisphosphate ($InsP_3$) sensors were created to follow intracellular $InsP_3$ changes in single living cells and in cell populations. Similar to previous $InsP_3$ sensors the new sensors are based on the ligand binding domain of the human type-I $InsP_3$ receptor ($InsP_3$R-LBD), but contain a mutation of either R265K or R269K to lower their $InsP_3$ binding affinity. Tagging the $InsP_3$R-LBD with N-terminal Cerulean and C-terminal Venus allowed measurement of $InsP_3$ in single-cell FRET experiments. Replacing Cerulean with a Luciferase enzyme allowed experiments in multi-cell format by measuring the change in the BRET signal upon stimulation. These sensors faithfully followed the agonist-induced increase in $InsP_3$ concentration in HEK 293T cells expressing the Gq-coupled AT1 angiotensin receptor detecting a response to agonist concentration as low as 10 pmol/L. Compared to the wild type $InsP_3$ sensor, the mutant sensors showed an improved off-rate, enabling a more rapid and complete return of the signal to the resting value of $InsP_3$ after termination of M3 muscarinic receptor stimulation by atropine. For parallel measurements of intracellular $InsP_3$ and Ca^{2+} levels in BRET experiments, the Cameleon D3 Ca^{2+} sensor was modified by replacing its CFP with luciferase. In these experiments depletion of plasma membrane PtdIns(4,5)P_2 resulted in the fall of $InsP_3$ level, followed by the decrease of the Ca^{2+}-signal evoked by the stimulation of the AT1 receptor. In contrast, when type-III PI 4-kinases were inhibited with a high concentration of wortmannin or a more specific inhibitor, A1, the decrease of the Ca^{2+}-signal preceded the fall of $InsP_3$ level indicating an $InsP_3$-, independent, direct regulation of capacitative Ca^{2+} influx by plasma membrane inositol lipids. Taken together, our results indicate that the improved $InsP_3$ sensor can be used to monitor both the increase and decrease of $InsP_3$ levels in live cells suitable for high-throughput BRET applications.

Introduction

Inositol-1,4,5-trisphosphate ($InsP_3$) plays a central role in calcium signaling. Its production is catalyzed by phospholipase C enzymes activated through receptor stimulation. Measurements of $InsP_3$ kinetics for a long time relied upon isotope labeling of cell populations followed by extraction and HPLC-separation of the active (1,4,5) isomer from the inactive (1,3,4) one [1]. Mass measurements of $InsP_3$ using radio-receptor assays have also been used [2] to measure absolute mass changes, again from populations of cell, but these methods have been quite cumbersome and unable to provide very detailed time resolution. Moreover, these methods did not allow detection of kinetic changes in single cells with accurate comparisons with other parameters, such as cytoplasmic Ca^{2+} changes. These deficiencies prompted several groups, including ours, to develop $InsP_3$ sensor that would be useful for single-cell analysis. With the advent of fluorescent proteins and the development of fluorescence resonance energy transfer (FRET) technology, $InsP_3$ probes based on the ligand binding domain of the $InsP_3$ receptor have been introduced and used successfully in several single-cell applications [3–7].

In reviewing our experimental data obtained with a sensor that was developed in our group (using the same principles referenced above) and comparing it with published sensors, such as IRIS [3], we noted that the sensors not only distorted $InsP_3$ kinetics because of their buffering effects (a complication that is unavoidable with any probe), but they also showed $InsP_3$ kinetics suggestive of slow off-rates. To overcome this problem, we designed modified probes to address these kinetic deficiencies. Importantly, we also wanted to take this tool further such that it could be used in cell populations allowing a format amenable to screening applications.

Here we report on the fine-tuning and characterization of our $InsP_3$ sensor based on the human type-I $InsP_3$ receptor LBD (residues 224–605). Structural studies showed that $InsP_3$ binding leads to a conformational change of this protein domain, which can be translated to a change in FRET signal between two appropriate fluorophores placed at the two ends of the LBD. Similar probes have been introduced and published (see Table 1). It has been show earlier that deletion of the N-terminal 223 amino acids increases the affinity of the LBD, so the 224–605 LBD has a higher affinity than the native $InsP_3$ receptor channel [8]. Therefore, we decided to engineer slightly lower affinity mutants by mutating the $InsP_3$ binding site in order to improve its off-rate upon decrease in $InsP_3$ but still keep their abilities to detect the increase of $InsP_3$ level. In addition, we have demonstrated the ability of these probes to faithfully monitor $InsP_3$ concentrations by either FRET or bioluminescence resonance energy transfer applications (BRET).

To analyze and compare our sensors, we needed an experimental system in which an increase or decrease in $InsP_3$ concentration could be equally established. For this, type-1 angiotensin receptor (AT1R) or the M3 cholinergic receptor was transiently transfected into HEK 293T cells, so that $InsP_3$ concentration could be increased by angiotensin II or carbachol stimulation, respectively. Decrease of $InsP_3$ was evoked by terminating the muscarinic response by atropine. Under these conditions both the wild-type and the mutant sensors were able to show the rapid rise in $InsP_3$ levels, but the mutants were able to detect a more rapid and full decline in $InsP_3$ concentration. Our data suggest that these improved mutant sensors are suitable to investigate $InsP_3$ signaling more accurately than previous ones either by single-cell imaging or in cell population measurements.

Table 1. InsP_3 sensors in use for single-cell fluorescent energy transfer-based applications.

Sensor	InsP_3-binding domain	K_D	Fluorescent proteins	Reference
LIBRA	rat type-III InsP_3R (1–604)	404 nM	CFP/YFP	[4, 31]
LIBRA-ΔN*	rat type-III InsP_3R (227–604)	ND	CFP/YFP	[4, 5, 31]
LIBRA-vI	rat type-I InsP_3R (1–604)	269 nM	CFP/Venus	[32]
LIBRA-vII	rat type-II InsP_3R (1–604)	234 nM	CFP/Venus	[32]
LIBRA-vIIS	LIBRAvII R440Q	117 nM	CFP/Venus	[32]
LIBRA-vIII	rat type-III InsP_3R (1–604)	492 nM	CFP/Venus	[5, 32]
LIBRA-vIIIS	LIBRAvIII R440Q	≈ 250 nM	CFP/Venus	[32]
Fretino	human type-I InsP_3R (224–579)	8 nM	CFP/YFP	[7]
Fretino-2	Fretino R504Q	190 nM	CFP/YFP	[7]
Fretino-3**	Fretino R508Q	ND	CFP/YFP	[7]
Fretino-4	human type-I InsP_3R (1–604)	ND	CFP/YFP	[7]
IRIS-1	mouse type-I InsP_3R (224–575)	549 nM (cell lysate), 437 nM (purified)	Venus/CFP	[3]
IRIS-1-Dmut**	IRIS-1 T276A, K508Q	ND		[3]
IRIS-1.2	IRIS-1 K249Q	3–4 μM		[3]
	mouse type-I InsP_3R (224–579)	95 nM	Venus/CFP	[3]
	mouse type-I InsP_3R (224–584)	105 nM	Venus/CFP	[3]
	mouse type-I InsP_3R (224–604)	107 nM	Venus/CFP	[3]
FIRE-1	rat type-I InsP_3R (1–589)	31 nM	CFP/YFP	[6]
FIRE-2	rat type-II InsP_3R (1–604)	ND	CFP/YFP	[6]
FIRE-3	rat type-III InsP_3R (1–604)	36 nM	CFP/YFP	[6]

K_D values represent the InsP_3 concentrations required to reach 50% of the dynamic range of the appropriate sensor. ND means not determined.

*InsP_3 insensitive mutant of LIBRA

**non-binding mutant for control experiments

doi:10.1371/journal.pone.0125601.t001

Materials and Methods

Materials

Molecular biology reagents were obtained from Fermentas (Vilnius, Lithuania). Cell culture dishes and plates were purchased from Greiner (Kremsmunster, Austria). Coelenterazine *h* was purchased from Regis Technologies (Morton Grove, IL). Lipofectamine 2000 was from Invitrogen (Carlsbad, CA). Rapamycin was obtained from Merck (Darmstadt, Germany). GeneCellin transfection reagent was from BioCellChallenge (Toulon, France). Atropine was purchased from EGIS (Budapest, Hungary). Unless otherwise stated, all other chemicals and reagents were purchased from Sigma (St Louis, MO).

DNA constructs

The R265K, R269K, R568K, R504K and R265,269K mutations were introduced by site-directed mutagenesis (Agilent Technologies, Santa Clara, CA USA) in the previously created mRFP-InsP_3R-LBD (residues 224–605 of human type-1 InsP_3 receptor S1+) construct used for bacterial expression of the fusion proteins [9]. To create the InsP_3 sensors first we made a FRET plasmid backbone by cloning the monomeric Venus [10] into the pEYFP-C1 plasmid, in which YFP was already replaced by Cerulean [11], using EcoRI and NotI enzymes. The wild type or mutant InsP_3R-LBDs were then inserted between the two fluorophores using XhoI and

EcoRI resulting in two short linkers before and after the LBD (NEQRSR and NS). From these FRET sensors the BRET sensors were prepared by replacing Cerulean with super *Renilla* luciferase [12]. To improve the optical parameters, another set of BRET sensors were created by replacing Venus with the Venus cp173-Venus tandem used in other sensors like the Epac cAMP sensor [13].

The Ca^{2+} sensor used in the BRET measurements was created by replacing the InsP_3R-LBD with the appropriate sequence derived from Cameleon D3 [14]. For the replacement, first this sequence was amplified using PCR with the sense primer CTCGAGACCAACTGACAGAA GAGCAGATTGCAGAG and antisense primer GAATTCAGTGCCCCGGAGCTGGAGA TCTTC, and then it was cloned into the BRET plasmid using XhoI and EcoRI enzymes.

Wild type human M3 cholinergic receptor (N-terminal 3x-hemagglutinin tagged) was purchased from S&T cDNA Resource Center (Rolla, MO). The non-internalizing rat type-I angiotensin receptor (AT1R-Δ319) was described earlier [15]. The plasma membrane targeted FRB-mRFP and mRFP-FKBP-5-ptase constructs used for rapamycin-induced PtdIns(4,5)P_2 depletion were described earlier [16] with the difference that for plasma membrane targeting of the FRB protein, we used the N-terminal targeting sequence (1–10) of mouse Lck (GenBank accession number: NM_001162433) [17].

Cell culture

HEK 293T and COS-7 cells (ATCC, Manassas, VA) were maintained in Dulbecco's modified Eagle's medium (DMEM, Lonza 12–604) supplemented with 10% fetal bovine serum, 50 U/ml penicillin and 50 μg/ml streptomycin in a 5% humidified CO_2 incubator at 37°C in 10 cm tissue culture plastic dishes.

InsP_3 binding experiments

mRFP-tagged wild type and mutant InsP_3R-LBD domains, built into the pET-23b bacterial expression vector (Novagen) were used to transform the BL-21 DE3 Star strain of *Escherichia coli* (Invitrogen). Bacterial cells were grown to A_{600} 0.6–0.9 at 37°C and induced with 300 μM isopropyl-1-thio-β-D-galactopyranoside at 18–20°C for 8 hours. Purification of the recombinant protein as well as InsP_3 binding assay were performed as described previously [9], using 0.75 μCi (1 nM) [^{3}H]Ins(1,4,5)P_3 (Amersham Biosciences) and 200 ng protein in an incubation volume of 50 μl.

Fluorescence Resonance Energy Transfer (FRET) measurements

For FRET measurements HEK 293T cells were trypsinized and plated on poly-lysine-pretreated (0.001%, 1 hour) No 1.5 glass coverslips in 35 mm plastic dishes at 3x10^5 cells/dish density. After one day the culture medium was changed to 1 ml Opti-MEM (Gibco) medium, and then 200 μl transfection solution containing the indicated DNA constructs (1 μg total DNA/dish) and 2 μl/dish Lipofectamine 2000 was added. After 6 hours 1 ml DMEM containing serum and antibiotics was added. Measurements were performed 24–32 hours after the transfection. Before the measurements the coverslips were placed into Attofluor cell chambers (Invitrogen) and the medium was changed to 800 μl of a modified Krebs–Ringer buffer containing 120 mM NaCl, 4.7 mM KCl, 1.2 mM $CaCl_2$, 0.7 mM $MgSO_4$, 10 mM glucose, and 10 mM Na-HEPES, pH 7.4. Measurements were performed at room temperature using an inverted microscope (Axio Observer D1, Zeiss, Germany) equipped with a 40x/1.3 oil-immersion objective (Plan-APO, Zeiss) and a Cascade II camera (Photometrics, Tucson, AZ). Excitation wavelengths (435 nm and 500 nm) were set by a monochromator connected to a 75 W Xenon lamp (DeltaRAM, Photon Technology International, Birmingham, NJ). The emitted light was

separated by a dichroic beamsplitter (Chroma 69008bs), and then detected through the appropriate emission filters for Cerulean (470/24 nm) and Venus (535/30 nm). Images were acquired every 5 s. The indicated reagents were also dissolved in modified Krebs–Ringer buffer and were added manually in 200 μl, and mixed three times. The MetaFluor (Molecular Devices, Downingtown, PA) software was used for data acquisition, whereas for further data analysis including background subtraction, bleed through correction and 535/470 emission ratio calculation the MetaMorph (Molecular Devices) software was applied.

Bioluminescence Resonance Energy Transfer (BRET) measurements

For BRET measurements HEK 293T cells were trypsinized and plated on poly-lysine-pretreated (0.001%, 1 hour) white 96-well plates at a density of 10^5 cells/well together with the indicated DNA constructs (0.24–0.3 μg total DNA/well) and the cell transfection reagent (0.5 μl/well Lipofectamine 2000 or 1.5 μl/well GeneCellin). After 6 hours 100 μl/well DMEM containing serum and antibiotics was added. Measurements were performed 24–27 h after transfection. Before measurements the medium of cells was changed to a medium (50 μl) containing 120 mM NaCl, 4.7 mM KCl, 1.2 mM $CaCl_2$, 0.7 mM $MgSO_4$, 10 mM glucose, and 10 mM Na-HEPES, pH 7.4. Measurements were performed at 37°C using a Mithras LB 940 multilabel reader (Berthold, Germany). The measurements started with the addition of the cell permeable luciferase substrate, coelenterazine *h* (40 μl, final concentration of 5 μM), and counts were recorded using 485 and 530 nm emission filters. Detection time was 500 ms for each wavelength. The indicated reagents were also dissolved in modified Krebs–Ringer buffer and were added manually in 10 μl. For this, plates were unloaded, which resulted in an interruption in the recordings. All measurements were done in triplicates. BRET ratios were calculated by dividing the 530 nm and 485 nm intensities, and normalized to the baseline.

Confocal microscopy

COS-7 cells were cultured on IBIDI μ-Slide 8 Well dishes (IBIDI GmbH, Cat. No.: 80826; $2x10^4$ cells/well) and transfected with the indicated constructs (1 μg DNA total/dish) using 0.5 μl/well Lipofectamine 2000 for 24 h. Confocal measurements were performed at 35°C in a modified Krebs-Ringer buffer described above, using a Zeiss LSM 710 scanning confocal microscope and a 63x/1.4 oil-immersion objective. Post-acquisition picture analysis was performed using the Photoshop (Adobe) software to expand to the full dynamic range but only linear changes were allowed.

Statistical analysis

To calculate the half-time values (τ) of the decay phase, a curve fitting procedure was applied to the values in each individual experiment using the 3 parametric exponential decay equation of ($y = y_0+ae^{-bx}$). τ values were then averaged and subjected to a t-test.

Results

Generation of reduced affinity InsP_3 sensors that can be used in energy transfer measurements

To design an improved InsP_3 sensor first we decided to perform a moderate modification in the InsP_3 binding domain (224–605 amino acids) of human type-I InsP_3 receptor (IP3R-LBD) [18] by replacing specific arginine residues to lysines. Since the side chain of lysine is shorter than that of arginine and lysine is a less basic amino-acid than arginine (pI-values are 9.74 and 10.76, respectively) we reasoned that interaction of the mutant protein with negatively charged

phosphate groups of InsP_3 will be weaker. We expected that this manipulation would decrease the binding affinity and therefore increase the off-rate performance of the sensor. Based on the crystal structure of the binding domain [19] we selected R265, R269, R504 and R568 residues for mutation (Fig 1A). To investigate the InsP_3 binding properties of these proteins, first we created constructs for bacterial expression. The mRFP-, and 6xHis-tagged InsP_3 binding domains were purified on Ni^{2+} columns, and in vitro binding assays were performed using [^{3}H] InsP_3 as the tracer. As shown in Fig 1B the binding of R265K, R269K and R568K were weaker compared to the wild type protein, while the R504K and the double mutant R265,269K were very poor InsP_3 binders. Scatchard analysis of the curves also showed the lower affinity of the mutants: the K_D value for the R265K, R269K and R568K mutants were 6.06 nM, 10.07 nM and 5.30 nM, respectively compared to 3.04 nM for the wild type LBD. Based on these results, the R265K and R269K mutants were selected for further analysis.

In previous studies we created the InsP_3R-LBD with various N-terminal fluorescent tags, such as mRFP or Cerulean, in combination with a C-terminal Venus tag. Application of the protein as InsP_3 sensor in BRET measurements requires that the N-terminal fluorescent protein tag be replaced with a luciferase enzyme. Fig 1C shows the final structure of the InsP_3 sensors that contain either Cerulean [11] or Super Luciferase (Sluc) [12] tag on their N-terminus, and Venus on the C-terminus. Studies on the dependence of energy transfer efficiency between fluorescent proteins suggested that introduction of double-acceptor moieties may significantly enhance the FRET efficiency value [13]. Therefore, we also created constructs with tandem yellow fluorescent tag (cp173 Venus and Venus) on their C-termini [13].

As shown before for the previously developed sensors, expression of these sensors in mammalian cells (COS-7 and HEK 293T) resulted in uniform cytoplasmic distribution of the fusion proteins and their reduced levels in the nucleus (Fig 1D). Similarly to other published InsP_3 sensors (see Table 1), InsP_3 binding caused a decrease of energy transfer in both FRET and BRET measurements (Fig 1E and 1F). Notably, duplication of the acceptor did not result in improvement of the signal in the BRET format (Fig 1F). Since raw BRET ratio values often show a spontaneous increase over time, we included wells that were left unstimulated and used these to correct for baseline drift. From these data the reciprocal of the I/I_0 values were calculated and plotted, therefore the elevation of cytoplasmic InsP_3 level corresponds to an increased value on the graphs. Since the BRET application is done in cell suspension and therefore inherently reports on averaged cell responses, the subsequent characterization was done using the BRET approach.

Characterization of the InsP_3 sensitivity and reversibility of the reduced affinity InsP_3 sensors

To compare the InsP_3-induced signals of the wild type and low affinity InsP_3 sensors, HEK 293T cells were transfected with the cDNAs of both the human AT1 receptor and the Sluc/Venus version of the appropriate InsP_3 sensor. BRET changes were then recorded following angiotensin II (Ang II) stimulation. As shown on Fig 2A, increasing concentrations of Ang II from 10^{-12} to 10^{-7} M resulted in an increasing BRET signal in case of both the wild type and the mutant sensors. The signals also showed a kinetic difference as the concentration of Ang II was increased (Fig 2A). While the maximal response was the same, a moderate shift to the right occurred on the dose-response curve in case of the sensor with the R265K mutation reflecting the lower affinity of this mutant sensor (Fig 2B).

To investigate the reversibility of the InsP_3 binding of the sensors, HEK 293T cells transiently expressing the M3 cholinergic receptor were stimulated first with carbachol (10 μM), which activated the Gq signaling pathway and elevated the cytoplasmic InsP_3 and Ca^{2+} levels. These

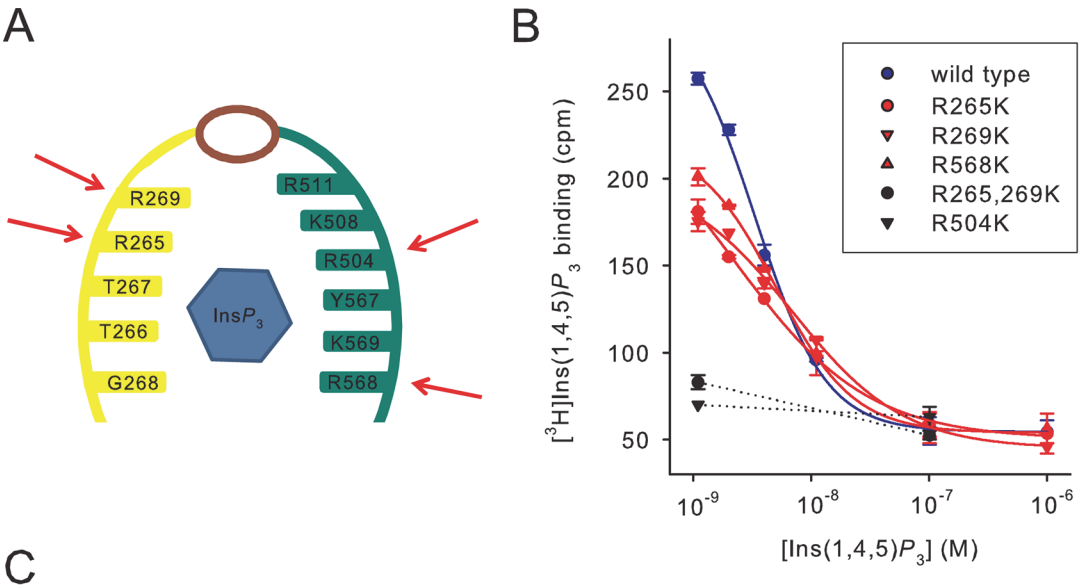
A
R269
R265
T267
T266
G268
InsP3
R511
K508
R504
Y567
K569
R568
B
wild type
R265K
R269K
R568K
R265,269K
R504K
[3H]Ins(1,4,5)P3 binding (cpm)
250
200
150
100
50
10-9
10-8
10-7
10-6
[Ins(1,4,5)P3] (M)

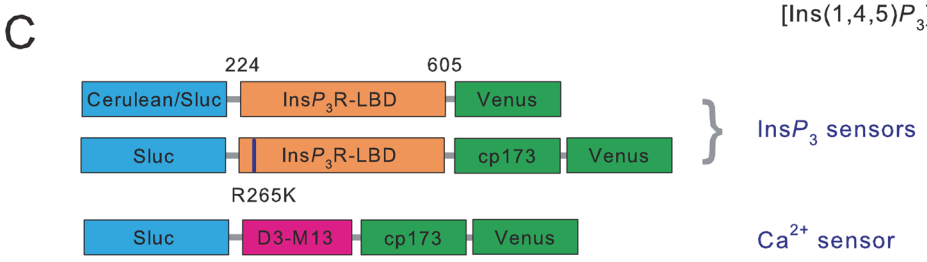
C
224
605
Cerulean/Sluc
InsP3R-LBD
Venus
Sluc
InsP3R-LBD
cp173
Venus
InsP3 sensors
R265K
Sluc
D3-M13
cp173
Venus
Ca2+ sensor

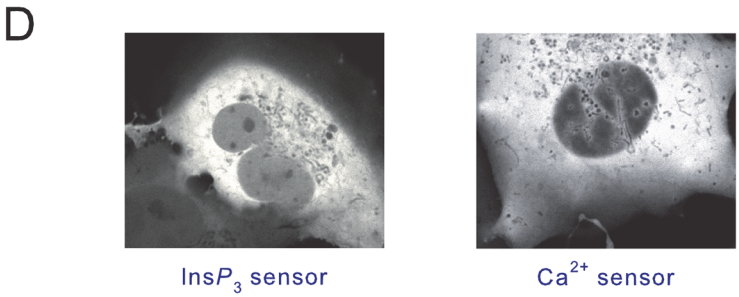
D
InsP3 sensor
Ca2+ sensor

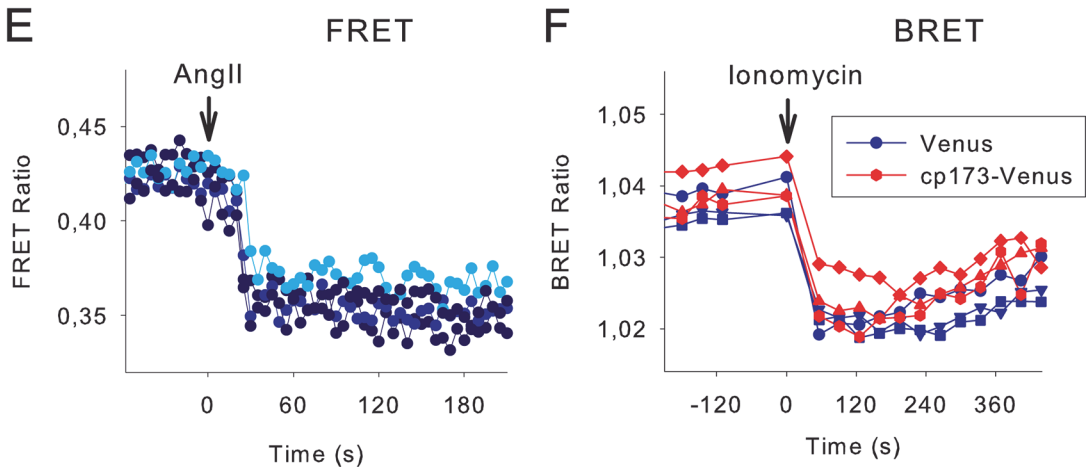
E
FRET
AngII
0,45
0,40
0,35
FRET Ratio
0
60
120
180
Time (s)
F
BRET
Ionomycin
Venus
cp173-Venus
1,05
1,04
1,03
1,02
BRET Ratio
-120
0
120
240
360
Time (s)

Fig 1. Characterization of the newly developed InsP_3 sensor. (A) Schematic drawing of the inositol 1,4,5-trisphosphate (InsP_3)-binding core domain based on its crystal structure [18]. Residues in the alpha helical domain and the beta-trefoil domain are highlighted in green and yellow, respectively. InsP_3 is highlighted in blue. The hinge region is shown in purple. Arginine to lysine mutations were introduced in the ligand binding residues at positions 265, 269, 504 and 568 (red arrows). (B) *In vitro* characterization of the inositol phosphate binding of recombinant mRFP-tagged InsP_3 binding domains. The assays were performed using [^{3}H]InsP_3 (see methods) in the presence of the indicated concentrations of the respective unlabeled ligand. Two separate experiments in triplicates. (C) Schematic representations of domain structures of the different InsP_3 biosensors and a modified Cameleon D3 BRET sensor for measuring the changes in cytoplasmic Ca^{2+} concentration. The InsP_3 sensors contain Cerulean (FRET) or Sluc (BRET) on the N-terminus, the ligand-binding domain of the human type-I InsP_3-receptor and either Venus or circularly permuted Venus (cp173) and Venus on the C-terminus. The blue lines show the approximate location of the designed mutations (R265K). The Ca^{2+} sensor contains the MLCK calmodulin binding peptide M13 and the D3 variant of calmodulin. (D) Representative images of InsP_3 or Ca^{2+} biosensor-containing COS-7 cells. (E) Measurements of FRET in individual HEK 293T cells expressing the FRET InsP_3 biosensor and the AT1 angiotensin receptor. InsP_3 production of the cells was triggered by 1 μM angiotensin II (Ang II). Note that binding of InsP_3 resulted in a decrease of the energy transfer. (F) Measurement of BRET in HEK 293T cells expressing two types of BRET InsP_3 biosensors containing a single or a tandem fluorescent protein (Venus or cp173-Venus and Venus). InsP_3 production was induced by ionomycin (10 μM). The curves indicate the raw BRET ratios of individual wells of a 96-well white tissue culture plate used in the BRET measurements.

doi:10.1371/journal.pone.0125601.g001

responses can be quickly terminated by adding the competitive antagonist atropine (10 μM). As shown in Fig 3A the rising phases of the signals, which reflect the elevation of InsP_3, were indistinguishable between the wild-type and mutant InsP_3 sensors (however, note the low temporal resolution of about 3 points per minute). In contrast, the mutant sensor showed a significantly enhanced off-rate (τ = 23.0±2.3 s) compared to the wild type sensor (τ = 44.9±7.5 s) (Mean ± S.E.M. n = 5, p = 0.024), and a complete return to the baseline. InsP_3 measurement performed with the wild-type sensor revealed an elevated level of cytoplasmic InsP_3 concentration after the atropine treatment, which may reflect an incomplete dissociation of InsP_3 from the high affinity wild-type sensor or a non-complete inhibition of M3R signaling with atropine. Notably, in control cells, which were not treated with atropine, the InsP_3 level remains elevated up to 10 minutes consistent with a slow desensitization of the M3R, as demonstrated previously [20].

Parallel measurements of cytoplasmic Ca^{2+} concentration, performed under the same experimental condition (in the same plate, but in cells that expressed the BRET version of a previously described low K_D Ca^{2+} sensor [14] instead of the InsP_3 sensors), revealed the termination of the Ca^{2+} signal upon atropine treatment with a kinetic, which was highly similar to the one showed by the mutant InsP_3 sensor (Fig 3B).

Parallel cytoplasmic InsP_3 and Ca^{2+} measurements suggest a role of phosphoinositides in the generation of capacitative Ca^{2+} entry

Having performed these control experiments we wanted to apply these new sensors to address some lingering questions in InsP_3/Ca^{2+} signaling. It has been widely accepted that a sustained elevation in cytoplasmic Ca^{2+} upon stimulation with a Ca^{2+}-mobilizing agonist is the consequence of emptying the intracellular Ca^{2+} stores, with a sequential activation of Ca^{2+} influx into the cells via the Ca^{2+} channel Orai1 [21]. However, the role of phosphoinositides has been raised not only as the source of InsP_3 but also as possible regulators of the capacitative Ca^{2+} entry process [22].

To investigate the role of inositol phospholipids and InsP_3 in this process, we performed parallel measurements of cytoplasmic InsP_3 and Ca^{2+} levels under conditions, where either the plasma membrane (PM) phosphatidylinositol 4,5-bisphosphate [PtdIns(4,5)P_2] level was rapidly reduced by the rapamycin-inducible PM PtdIns(4,5)P_2-depletion system (Fig 4A) or the PtdIns(4)P supply was decreased by wortmannin pretreatment (Fig 4D). To avoid the complicating effects of receptor desensitization, HEK 293T cells expressing the rapamycin-regulated phosphatase system were transfected with the cDNA of a C-terminally tail-deleted non-internalizing AT1 receptor mutant (AT1R-Δ319) [15]. As shown on Fig 4B, stimulation with Ang II resulted in a large and sustained increase in cytoplasmic InsP_3 levels, which was rapidly

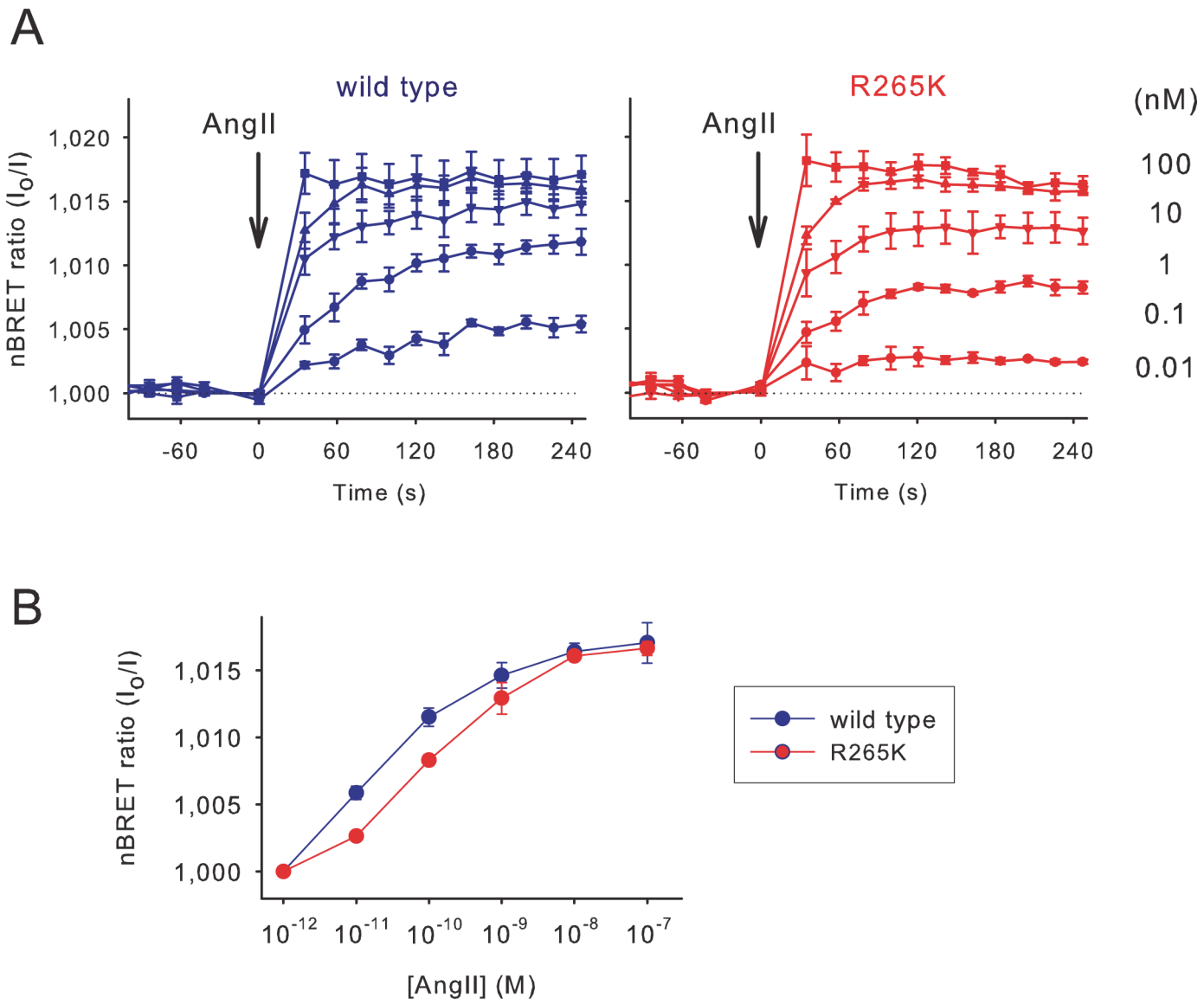

Fig 2. Comparison of the activation properties of the wild type and low-affinity InsP_3 sensors. (A) Normalized BRET ratio (reciprocal of I/I_0) measured in HEK 293T cells transiently transfected with the AT1 angiotensin receptor and the wild type or R265K mutant InsP_3 biosensors upon Ang II stimulation (10^{-12}-10^{-7} M) added manually. To avoid desensitization of the receptor a non-internalizing receptor was used (AT1R-Δ319). Error bars show standard error values from three independent measurements performed in triplicate. (B) Concentration-response curves for Ang II. InsP_3 responses were measured 5 minutes after stimulation. The right shift caused by the R265K mutation corresponds to the lower ligand binding affinity of the InsP_3 biosensor.

doi:10.1371/journal.pone.0125601.g002

terminated upon PtdIns(4,5)P_2 depletion evoked by rapamycin addition. The decay of the InsP_3 signal correlated well with the decline of the cytoplasmic Ca^{2+} level (Fig 4C) measured in parallel (side by side on the same plate) using the BRET version of the original Cameleon D3 Ca^{2+} sensor [14]. This correlation indicates that the newly developed InsP_3 sensor is suitable for monitoring the rapid termination of this signaling event.

Next we compared InsP_3 and Ca^{2+} kinetics following Ang II stimulation of cells pretreated with either 10 μM wortmannin or 10 nM A1, a recently published potent and more specific PI4KIIIα inhibitor [23]. Wortmannin at this concentration inhibits type-III PI4Ks (both α and β), thereby limiting the replenishment of the phosphoinositide pools [24]. As shown on Fig 4E,

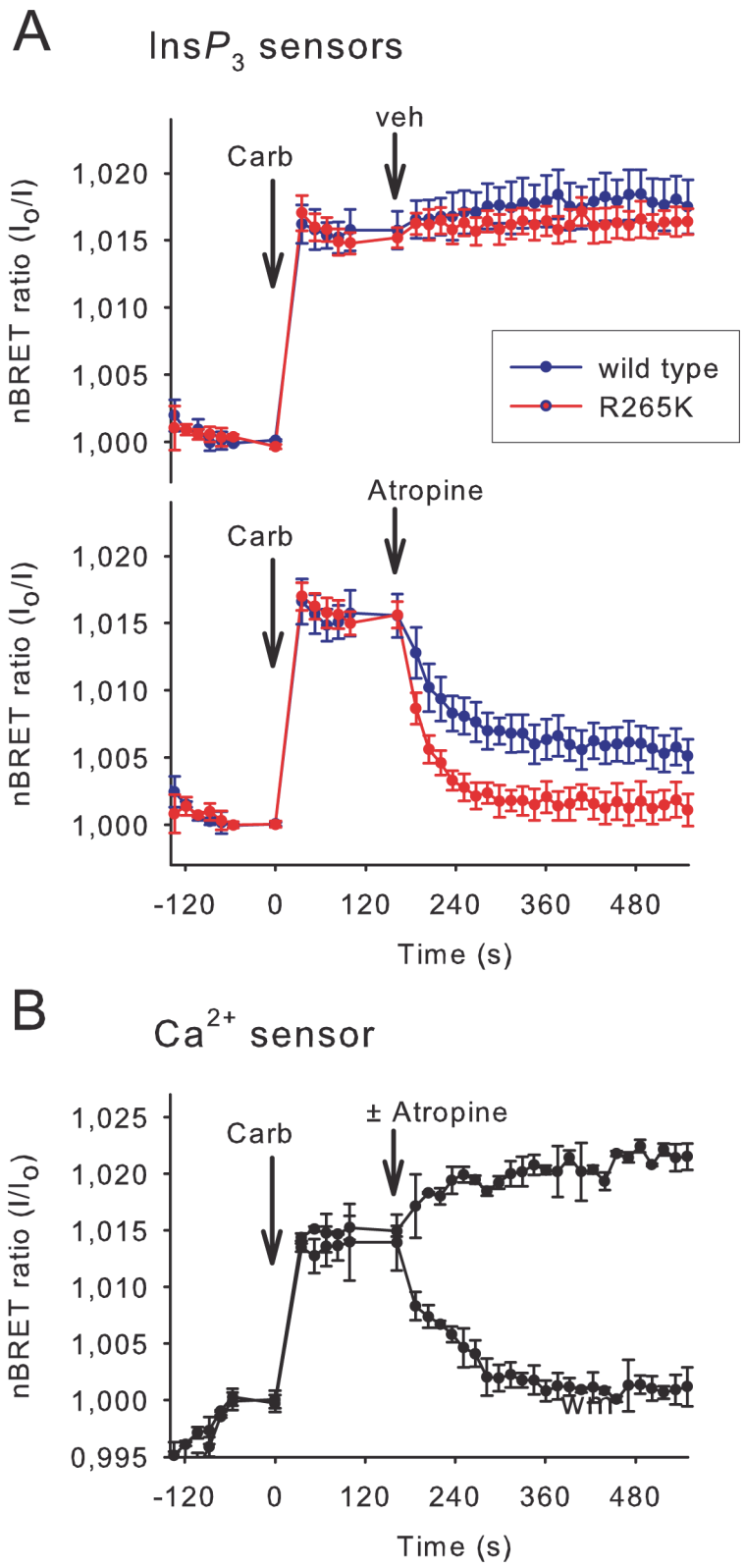

Fig 3. Comparison of the reversibility of the wild type and low-affinity InsP_3 sensors. (A) InsP_3 production was evoked in HEK 293T cells expressing the M3 cholinergic receptor and various BRET InsP_3 biosensors. Stimulation of the cells with 10 μM carbachol (Carb) added manually resulted in a maximal InsP_3

response sustained for at least 10 minutes (upper graph) as indicated by both the wild type and the R265K mutant InsP_3 biosensors. To examine how the biosensors can monitor the decrease of the InsP_3 signal the activation process was stopped by 10 μM atropine (lower graph) added manually, which caused the divergence of the curves corresponding to the wild type and R265K mutant InsP_3 biosensors. (B) Parallel measurement of the cytoplasmic Ca^{2+} level measured with the modified Cameleon D3 BRET sensor. Experiments were carried out on the same plate in parallel wells containing cells expressing the Ca^{2+} sensor instead of the InsP_3 sensors. Values are means ± SE of three independent experiments performed in triplicate.

doi:10.1371/journal.pone.0125601.g003

both the Ang II-evoked InsP_3 and Ca^{2+} responses became transient when cells were pretreated with 10 nM A1 or 10 μM wortmannin for 10 minutes before Ang II stimulation, whereas the initial increases were very similar. This is in agreement with the earlier observation using isotope-based InsP_3 measurements, in which wortmannin pretreatment greatly reduced resting PtdIns(4)P but only slightly affected the prestimulatory PtdIns(4,5)P_2 level [24]. However, strikingly, the decay in InsP_3 level was much slower than the decline in the Ca^{2+} levels after the pretreatment with PI4K inhibitors (Fig 4F). This suggested that the rapidly declining Ca^{2+} cannot be simply caused by the depletion of PtdIns(4,5)P_2 as a cause of declining InsP_3 and refilling of the endoplasmic reticulum (ER) Ca^{2+} stores. These results suggested that PI4K inhibition had an additional effect on Ca^{2+} signals, most likely on entry via the store-operated pathways.

Discussion

The purpose of the present studies was to develop an InsP_3 sensor that allows kinetic measurement of cytoplasmic InsP_3 concentration both in singe cells and in cell populations. The conformational change evoked by InsP_3 binding to the LBD domain of the InsP_3 receptor served as a rational basis for the development of various energy transfer-based InsP_3 sensors, summarized in Table 1. The evolution and evaluation of these sensors clearly showed that their InsP_3 binding affinity is a crucial factor in their suitability. While using the high affinity wild-type LBD domain in these applications makes the sensors very sensitive, their buffering effects and their slow off-rate has limited their use, especially in experiments where assessment of InsP_3 decreases was important. Several approaches have been used to modify the binding affinity of the LBD. For example, keeping the N-terminal inhibitory domain or truncation of the C-terminus of the LBD both reduced the binding affinity (Table 1). Mutations of amino acids responsible for the interaction with the InsP_3 ligand can either increase or decrease the affinity of ligand interaction. Unfortunately, the impact of such modifications often is too drastic and results in unsuitable sensors. In our studies the starting point was the binding domain (amino acids 224–605) of the human type-I InsP_3 receptor, which we previously used as a cytoplasmic InsP_3 buffer [25]. *In vitro* binding measurements performed with tritium-labelled InsP_3 resulted in an IC_{50} value of 4 nM for the ligand binding affinity of the GFP-tagged version of this domain [9], which is in good agreement with the 3 nM, calculated here from the Scatchard analysis for the ligand binding of the mRFP-tagged LBD. Since adding the N-terminal inhibitory domain led to a large drop in binding affinity (about one order of magnitude) [25], we attempted to make a more subtle change in the LBD, replacing key arginines within the InsP_3 binding site with lysines, trying to mimic the affinity close to that of the endogenous receptor. Among several mutants tested, the R265K and R269K mutants has proven to be suitable candidates for the development of improved InsP_3 sensors.

For FRET applications the wild type, R265K and R269K mutant LBDs were tagged with monomeric versions of Cerulean and Venus on their N- and C-termini, respectively. To make the sensor suitable for use in BRET measurements, we replaced Cerulean with Luciferase. The

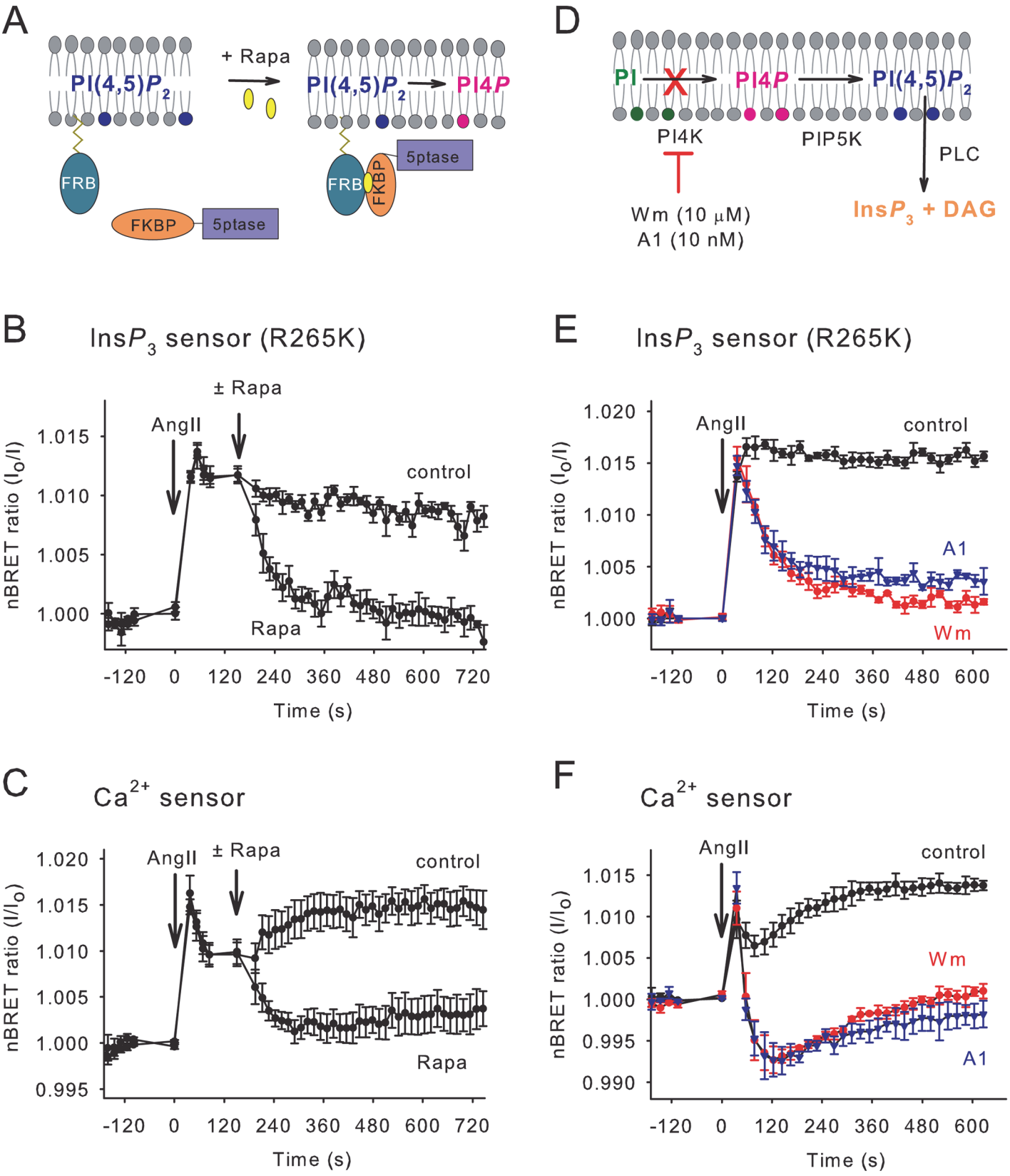
A
PI(4,5)P2
+ Rapa
PI(4,5)P2
PI4P
FRB
FKBP
5ptase
FRB
FKBP
5ptase
D
PI
PI4P
PI(4,5)P2
PI4K
PIP5K
PLC
Wm (10 μM)
A1 (10 nM)
InsP3 + DAG
B
InsP3 sensor (R265K)
± Rapa
AngII
control
Rapa
nBRET ratio (Io/I)
1.015
1.010
1.005
1.000
-120
0
120
240
360
480
600
720
Time (s)
E
InsP3 sensor (R265K)
AngII
control
A1
Wm
nBRET ratio (Io/I)
1.020
1.015
1.010
1.005
1.000
-120
0
120
240
360
480
600
Time (s)
C
Ca2+ sensor
AngII
± Rapa
control
Rapa
nBRET ratio (I/Io)
1.020
1.015
1.010
1.005
1.000
0.995
-120
0
120
240
360
480
600
720
Time (s)
F
Ca2+ sensor
AngII
control
Wm
A1
nBRET ratio (I/Io)
1.015
1.010
1.005
1.000
0.995
0.990
-120
0
120
240
360
480
600
Time (s)

Fig 4. Reduction of plasma membrane PtdIns(4)*P* and PtdIns(4,5)P_2 levels and their effect on the InsP_3 and Ca^{2+} signals upon hormonal stimulation. (A) Schematic representation of the plasma membrane PtdIns(4,5)P_2 depletion system [33]. Addition of rapamycin induces the heterodimerization of the FRB and FKBP domains in PM-FRB and FKBP-5ptase and thus causes the translocation of the latter molecule to the plasma membrane where it degrades PtdIns(4,5)P_2. (B and C) HEK 293T cells were transiently transfected with AT1R-Δ319 together with the PtdIns(4,5)P_2 depleting system and the indicated BRET sensors. After hormonal stimulation (100 nM Ang II), 300 nM rapamycin was added manually to cause acute depletion of PtdIns(4,5)P_2 in the PM. (means ± SE, n = 4). (D) During the synthesis of PtdIns(4,5)P_2, first the PI4K enzymes phosphorylate PI, and then PIP5K produces PtdIns(4,5)P_2 from PtdIns(4)*P*. The plasma membrane PtdIns(4)*P* content can be depleted by preincubation of the cells with the selective PI4KIIIα inhibitor, A1 or a high concentration of wortmannin (Wm). (E and F) HEK 293T cells were transiently transfected with AT1R-Δ319 together with the indicated BRET sensors. A 10-minute preincubation with 10 μM wortmannin or 10 nM A1 was used to decrease the PtdIns(4)*P* level of the PM. The curves show the changes in the normalized BRET ratio (means ± SE, n = 3) of the indicated sensors upon manual addition of 100 nM Ang II.

doi:10.1371/journal.pone.0125601.g004

advantage of BRET measurement over FRET is that it can be carried out in simple plate readers and that it shows the average change in a cell population. Since it does not require excitation, there is no crosstalk between the emission channels. Therefore, energy transfer can be followed by simply calculating the emission ratio without any correction. Data processing is reduced only to taking the reciprocal of the ratio values to obtain an increase when InsP_3 level elevates, and normalizing the data to the resting values. Replacement of Venus with a double Venus construct (Venus cp173-Venus) did not yield further benefits either in the FRET or BRET format. Our mutant InsP_3 sensors tested in BRET applications showed a slightly reduced but still high sensitivity to agonist stimulation, while they performed better when the decay of InsP_3 was followed after termination of InsP_3 production. This was either achieved by terminating receptor stimulation or rapidly removing PtdIns(4,5)P_2, the precursor of InsP_3. This allowed us to perform specific experiments to test the utility of these sensors to address questions regarding the connection between InsP_3 and Ca^{2+} entry regulation.

It has been shown previously that pretreatment of cells with concentrations of wortmannin, that inhibit PI3- and PI4-kinases, modifies the shape of the agonist-evoked Ca^{2+} signal by eliminating its sustained elevation [24, 26]. This was initially attributed to the fact that wortmannin limits the replenishment of the plasma membrane phosphoinositide pools by inhibiting type-III PI4Ks, therefore leading to the run-down of these lipids during agonist stimulation [24]. Since Ca^{2+} influx through the capacitative Ca^{2+} entry pathway is regulated by the ER luminal Ca^{2+} concentration, which in turn, is controlled by the opening of the InsP_3 receptor channels in the ER, it was logical to assume that the falling InsP_3 levels in wortmannin-treated cells would allow ER Ca^{2+} pools to refill and shut down the store-operated Ca^{2+} entry process. In fact, it has been shown by early studies that Icrac (the current that corresponds to store-regulated Ca^{2+} entry) is inhibited by wortmannin [27]. Subsequent studies performed after the identification of the molecules responsible for SOCE, have also indicated that phosphoinositides in the plasma membrane may directly influence this Ca^{2+} entry route either by affecting the Orai channels or the ER-sensor STIM1 molecule [22, 28–30].

Our new ability of monitoring InsP_3 and Ca^{2+} changes allowed us to address this question in a way that relied upon endogenous levels of STIM1 and Orai1.

We compared the decay kinetics of Ca^{2+} and InsP_3 either after rapidly removing PtdIns(4,5)P_2 or limiting phosphoinositide supplies by wortmannin (or now the more specific PI4KIIIa inhibitor, A1) pretreatment. We found a significant difference between the two manipulations: while the InsP_3 and Ca^{2+} decreases were parallel after PtdIns(4,5)P_2 depletion, the Ca^{2+} decrease was substantially faster than that of InsP_3 in the PI4K inhibitor pretreated cells. This suggested that PI4KIIIa inhibition exerted an additional effect on Ca^{2+} signaling. that was different from a simple PtdIns(4,5)P_2 depletion evoked by the PM-recruited 5-ptase.

The most important difference between the two manipulations is the change in the level of plasma membrane PtdIns(4)*P*. While PtdIns(4,5)P_2 elimination by the 5-ptase increases PtdIns(4)*P* levels, A1 or wortmannin pretreatment selectively depletes PtdIns(4)*P* even before

agonist stimulation and PtdIns(4,5)P_2 decreases only occur after agonist addition. All of these argue for a role for PtdIns(4)P or a mechanism sensitive to its level in playing a role in the control of store-operated Ca^{2+} entry. These conclusions were consistent with those of earlier reports using different approaches [22, 27].

We also observed a peculiar decrease of the Ca^{2+} levels below the prestimulatory values when cells were stimulated after PI4K inhibition. While this may be a feature brought out by our genetically encoded Ca^{2+} sensor, it raised the possibility that Ca^{2+} extrusion is also stimulated by agonists and together with inhibition of Ca^{2+} entry due to the simultaneous elimination of both PtdIns(4)P and PtdIns(4,5)P_2 manifests in a Ca^{2+} decrease below basal. Further exploration of this possibility, however, was beyond the scope of this study.

In summary, in this paper we described and characterized an improved InsP_3 sensor which is based on the ligand binding domain of human type-1 InsP_3 receptor but contains the R265K mutation. While this sensor maintains its sensitivity and can be used to monitor small increases of cytoplasmic InsP_3 concentration, it also has an improved off-rate to follow the decrease of the InsP_3 level. While the sensor also works in FRET applications, an important new feature was its adaptation for BRET applications usable in plate readers to support high-throughput measurement of cytoplasmic InsP_3 in live cells alone, or in combination with measurements of other signaling factors, such as cytoplasmic Ca^{2+} concentration.

Acknowledgments

P. V. was supported by the Hungarian Scientific Research Fund (OTKA K105006). T.B. was supported by the Intramural Research Program of the Eunice Kennedy Shriver National Institute of Child Health and Human Development of the National Institutes of Health. The technical assistance of Kata Szabolcsi is highly appreciated.

Author Contributions

Conceived and designed the experiments: IK TB PV. Performed the experiments: GG JTT PV. Analyzed the data: GG JTT TB PV. Contributed reagents/materials/analysis tools: LH. Wrote the paper: DJT IK LH TB PV.

References

1. Balla T, Baukal AJ, Guillemette G, Morgan RO, Catt KJ. Angiotensin-stimulated production of inositol trisphosphate isomers and rapid metabolism through inositol 4-monophosphate in adrenal glomerulosa cells. Proceedings of the National Academy of Sciences of the United States of America. 1986; 83 (24):9323–7. Epub 1986/12/01. PMID: 3025836; PubMed Central PMCID: PMC387130.
2. Bredt DS, Mourey RJ, Snyder SH. A simple, sensitive, and specific radioreceptor assay for inositol 1,4,5-trisphosphate in biological tissues. Biochemical and biophysical research communications. 1989; 159(3):976–82. Epub 1989/03/31. PMID: 2539157.
3. Matsu-ura T, Michikawa T, Inoue T, Miyawaki A, Yoshida M, Mikoshiba K. Cytosolic inositol 1,4,5-trisphosphate dynamics during intracellular calcium oscillations in living cells. The Journal of cell biology. 2006; 173(5):755–65. Epub 2006/06/07. doi: 10.1083/jcb.200512141 PMID: 16754959; PubMed Central PMCID: PMC2063891.
4. Nezu A, Tanimura A, Morita T, Shitara A, Tojyo Y. A novel fluorescent method employing the FRET-based biosensor "LIBRA" for the identification of ligands of the inositol 1,4,5-trisphosphate receptors. Biochimica et biophysica acta. 2006; 1760(8):1274–80. Epub 2006/06/17. doi: 10.1016/j.bbagen.2006.04.004 PMID: 16777332.
5. Nezu A, Tanimura A, Morita T, Tojyo Y. Visualization of Ins(1,4,5)P3 dynamics in living cells: two distinct pathways for Ins(1,4,5)P3 generation following mechanical stimulation of HSY-EA1 cells. Journal of cell science. 2010; 123(Pt 13):2292–8. Epub 2010/06/18. doi: 10.1242/jcs.064410 PMID: 20554898.
6. Remus TP, Zima AV, Bossuyt J, Bare DJ, Martin JL, Blatter LA, et al. Biosensors to measure inositol 1,4,5-trisphosphate concentration in living cells with spatiotemporal resolution. The Journal of biological chemistry. 2006; 281(1):608–16. Epub 2005/10/27. doi: 10.1074/jbc.M509645200 PMID: 16249182.

7. Sato M, Ueda Y, Shibuya M, Umezawa Y. Locating inositol 1,4,5-trisphosphate in the nucleus and neuronal dendrites with genetically encoded fluorescent indicators. Analytical chemistry. 2005; 77 (15):4751–8. Epub 2005/08/02. doi: 10.1021/ac040195j PMID: 16053285.
8. Yoshikawa F, Iwasaki H, Michikawa T, Furuichi T, Mikoshiba K. Cooperative formation of the ligand-binding site of the inositol 1,4, 5-trisphosphate receptor by two separable domains. The Journal of biological chemistry. 1999; 274(1):328–34. PMID: 9867847.
9. Varnai P, Lin X, Lee SB, Tuymetova G, Bondeva T, Spat A, et al. Inositol lipid binding and membrane localization of isolated pleckstrin homology (PH) domains. Studies on the PH domains of phospholipase C delta 1 and p130. The Journal of biological chemistry. 2002; 277(30):27412–22. doi: 10.1074/jbc.M109672200 PMID: 12019260.
10. Nagai T, Ibata K, Park ES, Kubota M, Mikoshiba K, Miyawaki A. A variant of yellow fluorescent protein with fast and efficient maturation for cell-biological applications. Nature biotechnology. 2002; 20(1):87–90. doi: 10.1038/nbt0102-87 PMID: 11753368.
11. Rizzo MA, Springer GH, Granada B, Piston DW. An improved cyan fluorescent protein variant useful for FRET. Nature biotechnology. 2004; 22(4):445–9. doi: 10.1038/nbt945 PMID: 14990965.
12. Woo J, von Arnim AG. Mutational optimization of the coelenterazine-dependent luciferase from Renilla. Plant methods. 2008; 4:23. doi: 10.1186/1746-4811-4-23 PMID: 18826616; PubMed Central PMCID: PMC2565673.
13. van der Krogt GN, Ogink J, Ponsioen B, Jalink K. A comparison of donor-acceptor pairs for genetically encoded FRET sensors: application to the Epac cAMP sensor as an example. PloS one. 2008; 3(4): e1916. doi: 10.1371/journal.pone.0001916 PMID: 18382687; PubMed Central PMCID: PMC2271053.
14. Palmer AE, Giacomello M, Kortemme T, Hires SA, Lev-Ram V, Baker D, et al. Ca2+ indicators based on computationally redesigned calmodulin-peptide pairs. Chemistry & biology. 2006; 13(5):521–30. doi: 10.1016/j.chembiol.2006.03.007 PMID: 16720273.
15. Hunyady L, Bor M, Balla T, Catt KJ. Identification of a cytoplasmic Ser-Thr-Leu motif that determines agonist-induced internalization of the AT1 angiotensin receptor. The Journal of biological chemistry. 1994; 269(50):31378–82. PMID: 7989302.
16. Toth DJ, Toth JT, Gulyas G, Balla A, Balla T, Hunyady L, et al. Acute depletion of plasma membrane phosphatidylinositol 4,5-bisphosphate impairs specific steps in endocytosis of the G-protein-coupled receptor. Journal of cell science. 2012; 125(Pt 9):2185–97. doi: 10.1242/jcs.097279 PMID: 22357943; PubMed Central PMCID: PMC3367940.
17. Rodgers W. Making membranes green: construction and characterization of GFP-fusion proteins targeted to discrete plasma membrane domains. BioTechniques. 2002; 32(5):1044–6, 8, 50–1. PMID: 12019777.
18. Mikoshiba K. IP3 receptor/Ca2+ channel: from discovery to new signaling concepts. Journal of neurochemistry. 2007; 102(5):1426–46. Epub 2007/08/19. doi: 10.1111/j.1471-4159.2007.04825.x PMID: 17697045.
19. Bosanac I, Alattia JR, Mal TK, Chan J, Talarico S, Tong FK, et al. Structure of the inositol 1,4,5-trisphosphate receptor binding core in complex with its ligand. Nature. 2002; 420(6916):696–700. Epub 2002/11/21. doi: 10.1038/nature01268 PMID: 12442173.
20. Torrecilla I, Spragg EJ, Poulin B, McWilliams PJ, Mistry SC, Blaukat A, et al. Phosphorylation and regulation of a G protein-coupled receptor by protein kinase CK2. The Journal of cell biology. 2007; 177 (1):127–37. Epub 2007/04/04. doi: 10.1083/jcb.200610018 PMID: 17403928; PubMed Central PMCID: PMC2064117.
21. Varnai P, Hunyady L, Balla T. STIM and Orai: the long-awaited constituents of store-operated calcium entry. Trends in pharmacological sciences. 2009; 30(3):118–28. doi: 10.1016/j.tips.2008.11.005 PMID: 19187978; PubMed Central PMCID: PMC3125588.
22. Korzeniowski MK, Popovic MA, Szentpetery Z, Varnai P, Stojilkovic SS, Balla T. Dependence of STIM1/Orai1-mediated calcium entry on plasma membrane phosphoinositides. The Journal of biological chemistry. 2009; 284(31):21027–35. doi: 10.1074/jbc.M109.012252 PMID: 19483082; PubMed Central PMCID: PMC2742867.
23. Bojjireddy N, Botyanszki J, Hammond G, Creech D, Peterson R, Kemp DC, et al. Pharmacological and genetic targeting of the PI4KA enzyme reveals its important role in maintaining plasma membrane phosphatidylinositol 4-phosphate and phosphatidylinositol 4,5-bisphosphate levels. The Journal of biological chemistry. 2014; 289(9):6120–32. Epub 2014/01/15. doi: 10.1074/jbc.M113.531426 PMID: 24415756; PubMed Central PMCID: PMC3937678.
24. Nakanishi S, Catt KJ, Balla T. A wortmannin-sensitive phosphatidylinositol 4-kinase that regulates hormone-sensitive pools of inositolphospholipids. Proceedings of the National Academy of Sciences of the United States of America. 1995; 92(12):5317–21. Epub 1995/06/06. PMID: 7777504; PubMed Central PMCID: PMC41685.

25. Varnai P, Balla A, Hunyady L, Balla T. Targeted expression of the inositol 1,4,5-triphosphate receptor (IP3R) ligand-binding domain releases Ca2+ via endogenous IP3R channels. Proceedings of the National Academy of Sciences of the United States of America. 2005; 102(22):7859–64. doi: 10.1073/pnas.0407535102 PMID: 15911776; PubMed Central PMCID: PMC1142351.

26. Balla A, Kim YJ, Varnai P, Szentpetery Z, Knight Z, Shokat KM, et al. Maintenance of hormone-sensitive phosphoinositide pools in the plasma membrane requires phosphatidylinositol 4-kinase IIIalpha. Molecular biology of the cell. 2008; 19(2):711–21. doi: 10.1091/mbc.E07-07-0713 PMID: 18077555; PubMed Central PMCID: PMC2230591.

27. Broad LM, Braun FJ, Lievremont JP, Bird GS, Kurosaki T, Putney JW Jr. Role of the phospholipase C-inositol 1,4,5-trisphosphate pathway in calcium release-activated calcium current and capacitative calcium entry. The Journal of biological chemistry. 2001; 276(19):15945–52. doi: 10.1074/jbc.M011571200 PMID: 11278938.

28. Calloway N, Owens T, Corwith K, Rodgers W, Holowka D, Baird B. Stimulated association of STIM1 and Orai1 is regulated by the balance of PtdIns(4,5)P(2) between distinct membrane pools. Journal of cell science. 2011; 124(Pt 15):2602–10. doi: 10.1242/jcs.084178 PMID: 21750194; PubMed Central PMCID: PMC3138702.

29. Maleth J, Choi S, Muallem S, Ahuja M. Translocation between PI(4,5)P2-poor and PI(4,5)P2-rich microdomains during store depletion determines STIM1 conformation and Orai1 gating. Nat Commun. 2014; 5:5843. Epub 2014/12/18. doi: 10.1038/ncomms6843 PMID: 25517631; PubMed Central PMCID: PMC4270102.

30. Walsh CM, Chvanov M, Haynes LP, Petersen OH, Tepikin AV, Burgoyne RD. Role of phosphoinositides in STIM1 dynamics and store-operated calcium entry. The Biochemical journal. 2010; 425 (1):159–68. Epub 2009/10/22. doi: 10.1042/BJ20090884 PMID: 19843011; PubMed Central PMCID: PMC2860680.

31. Tanimura A, Nezu A, Morita T, Turner RJ, Tojyo Y. Fluorescent biosensor for quantitative real-time measurements of inositol 1,4,5-trisphosphate in single living cells. The Journal of biological chemistry. 2004; 279(37):38095–8. Epub 2004/07/24. doi: 10.1074/jbc.C400312200 PMID: 15272011.

32. Tanimura A, Morita T, Nezu A, Shitara A, Hashimoto N, Tojyo Y. Use of Fluorescence Resonance Energy Transfer-based Biosensors for the Quantitative Analysis of Inositol 1,4,5-Trisphosphate Dynamics in Calcium Oscillations. The Journal of biological chemistry. 2009; 284(13):8910–7. Epub 2009/01/23. doi: 10.1074/jbc.M805865200 PMID: 19158094; PubMed Central PMCID: PMC2659248.

33. Varnai P, Thyagarajan B, Rohacs T, Balla T. Rapidly inducible changes in phosphatidylinositol 4,5-bisphosphate levels influence multiple regulatory functions of the lipid in intact living cells. The Journal of cell biology. 2006; 175(3):377–82. doi: 10.1083/jcb.200607116 PMID: 17088424; PubMed Central PMCID: PMC2064515.